DOI: 10.1002/ejic.200900472

Nickel-Assisted Oxidative C–C Coupling and Subsequent Cleavage to C=O of Active Methylene Group in a Tetradentate Ligand System: Di- and Mononuclear Complexes with Transformed Ligands

Abhik Mukhopadhyay[a] and Samudranil Pal*[a]

Keywords: Nickel / Ligand transformation / C–C coupling / Structure elucidation / EPR spectroscopy / Magnetic properties

Treatment of pyrazolines (isolated or prepared in situ from 4-R-benzoylhydrazines and acetylacetone in a 2:1 mol ratio) with $Ni(O_2CCH_3)_2{\cdot}4H_2O$ in boiling methanol results in the formation of nickel(II) complexes of formula [Ni(H^RL)] [**1** (R = H) and **2** (R = OMe)], where $(H^RL)^{2-}$ represents the deprotonated Schiff base acetylacetone bis(4-R-benzoylhydrazone). Despite several attempts, the analogous nickel(II) complex with R = NMe_2 could not be isolated. However, stirring the above described reaction mixtures in air at room temperature for approximately 5 h provides dinuclear paramagnetic species [Ni(^RL–^RL)Ni] [**3** (R = H), **4** (R = OMe), and **5** (R = NMe_2)]. Here $(^RL–^RL)^{6-}$ represents the dinucleating ligand formed by oxidative C–C coupling involving the central methylene group of the acetylacetone fragment of $(H^RL)^{2-}$. The room-temperature (300 K) magnetic moments of **3**–**5** indicate an $S = 1/2$ spin state of each metal center in these dinuclear complexes. Cryomagnetic measurements with **3** reveal its weak antiferromagnetic nature. The EPR spectral features suggest that **3**–**5** are on the borderline between genuine nickel(III) species and nickel(II)-stabilized ligand radical systems. In wet dichloromethane/hexane mixture under aerobic conditions, each of **3**–**5** forms mononuclear nickel(II) complexes of formula [Ni(^RLO)] [**6** (R = H), **7** (R = OMe), and **8** (R = NMe_2)], where $(^RLO)^{2-}$ represents the tetradentate ligand formed from $(^RL–^RL)^{6-}$ by C–C bond cleavage followed by oxidation to the keto group. The molecular structures of **1**, **2**, **5**, **7**, and **8**, determined by X-ray crystallography, are reported.

Introduction

Interest in the chemistry of trivalent nickel is largely due to its potential/proven roles in catalytic oxidation reactions and some biological processes.[1] A variety of authentic complexes of nickel(III) with ligands containing different types of high-oxidation-state-promoting functionalities are reported in the literature.[2,3] One of these functionalities is the nitrogen-coordinating deprotonated amide, which is well known in stabilizing higher-valent transition-metal ions.[3] We have been working on coordination complexes of tridentate acyl- and aroylhydrazones, which contain the O-coordinating amide functionality.[4] Recently, in our attempt to prepare acetylacetone bis(benzoylhydrazone) (H_3L) (Scheme 1), we have isolated a cyclized product, 1-benzoyl-3,5-dimethyl-5-(1′-benzoylhydrazido)pyrazoline (bzpyzn).[5] Formation of such pyrazoline derivatives from semicarbazides/thiosemicarbazides or related species and 1,3-diketones is not uncommon.[6] Reactions of metal acetates with the pyrazoline derived from acetylacetone and thiosemicarbazide (1:2 mol ratio) under anaerobic conditions results in ring opening and formation of complexes having the formula [M(HL^1)] [M = Cu^{II} and Zn^{II}, H_3L^1 = acetylacetone bis(thiosemicarbazone)].[6d,7] However, under aerobic conditions, the active methylene group of the ligand in [M(HL^1)] is oxidized to a keto group and complexes of formula [M(L^1O)] have been isolated (Scheme 1).[6d,7] There is no report on the nature of the intermediate involved in the conversion of [M(HL^1)] to [M(L^1O)]. On the other hand, mononuclear [Ni(HL^2)] complexes with a very similar ligand system, acetylacetone bis(S-alkylisothiosemicarbazone) (H_3L^2), on oxidation provide a paramagnetic dinuclear species of formula [Ni(L^2–L^2)Ni] (Scheme 1). Here, $(HL^2)^{2-}$ is transformed to the dinucleating ligand $(L^2–L^2)^{6-}$ by oxidative C–C coupling.[8] There is no further report on the reactivity or formation of any other product from [Ni(L^2–L^2)Ni]. In our previous work,[5] we could not prepare [Ni(HL)], but we found that the reaction of bzpyzn with nickel acetate in the presence of air provides a green paramagnetic species. On the basis of the magnetic moment, EPR spectral features, and other physical properties, we had proposed an empirical formula, [Ni(L)], for this paramagnetic complex, which is on the borderline between a nickel(III) species and a nickel(II)-stabilized ligand radical species. It may be noted that a divanadium(IV) complex, $[V_2(L)_2(\mu\text{-PhCONNCOPh})]$, with the same ligand $(L)^{3-}$ and the bridging, doubly deprotonated *N*,*N*′-dibenzoylhydrazine, was reported before.[9] In the same report, a dinuclear oxovanadium(IV) complex, [OV(HL–LH)VO] (Scheme 1),

[a] School of Chemistry, University of Hyderabad, Hyderabad 500046, India
E-mail: spsc@uohyd.ernet.in

prepared by reacting $[VCl_2(acpn)]$ [acpn = propylenediiminobis(acetylacetonate)] with benzoylhydrazine was also described.[9] Here, $(HL–LH)^{4–}$ represents the $2H^+/2e^–$ oxidation product from two $(HL)^{2–}$. In solution under wet conditions, the green paramagnetic nickel complex transforms to a diamagnetic nickel(II) complex of formula [Ni(LO)], in which the central methylene group of $(HL)^{2–}$ is converted to a keto group.[5] We have further investigated the nickel chemistry with this tetradentate ligand system by using benzoylhydrazine as well as 4-R-benzoylhydrazines (R = OMe and NMe_2) for a better understanding of the identity of the paramagnetic species [Ni(L)] and its precursor. We have been able to isolate the precursor diamagnetic nickel(II) species $[Ni(H^RL)]$, and the paramagnetic complex from it is found to be a dinuclear species of formula $[Ni(^RL–^RL)Ni]$ instead of $[Ni(^RL)]$. These dinuclear complexes produce $[Ni(^RLO)]$ under wet conditions as a result of the cleavage of the bridging C–C bond followed by formation of C=O bonds (Scheme 1). Herein we give a detailed report on the syntheses, structures, and physical properties of these complexes. The present results, together with the observations previously reported by us and others,[5,6d,7–9] provide a comprehensive picture regarding the coordination chemistry of this class of tetradentate Schiff base ligands.

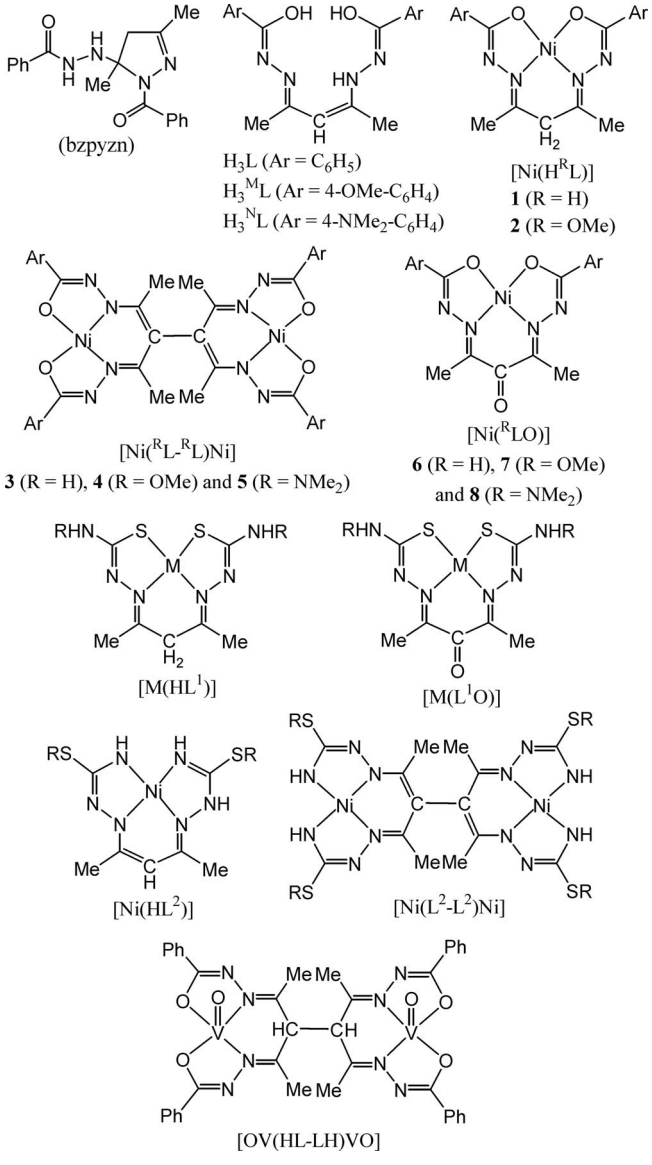

Scheme 1. Ligands used and nickel complexes described in this study with related species reported before.

Results and Discussion

Synthesis and Characterization

Reactions of $Ni(O_2CCH_3)_2·4H_2O$ with pyrazolines (isolated or prepared in situ from acetylacetone and 4-R-benzoylhydrazine in a 1:2 mol ratio) in methanol under reflux provide the brown crystalline nickel(II) complexes of general formula $[Ni(H^RL)]$ [**1** (R = H) and **2** (R = OMe)]. However, we could not isolate the analogous complex with R = NMe_2. Interestingly, when the reaction mixtures were stirred in air instead of being subjected to reflux, dinuclear complexes of general formula $[Ni(^RL–^RL)Ni]$ [**3** (R = H), **4** (R = OMe), and **5** (R = NMe_2)] were isolated. It is very likely that prolonged exposure to oxygen in air during the stirring helps the formation of $[Ni(^RL–^RL)Ni]$ instead of $[Ni(H^RL)]$, which are isolated in a closed atmosphere having limited exposure to air. It may be noted that the treatment of methanol solutions of **1** and **2** with H_2O_2 immediately provides **3** and **4**, respectively. The color of both **3** and **4** is green, while that of **5** is purple. In wet dichloromethane/hexane solution, **3**, **4**, and **5** are transformed to brown mononuclear nickel(II) complexes **6**, **7**, and **8**, respectively. These species have the general formula $[Ni(^RLO)]$. Formation of $[Ni(^RLO)]$ occurs only when both moisture and air oxygen are present. None of the complexes (**1**–**8**) conducts electricity in solution. The elemental analysis data and the non-electrolytic behavior of **1**–**8** are consistent with their molecular formulae mentioned above.

In the infrared spectra of **1**–**5**, there are no bands attributable to an N–H group or a C=O group. The absence of N–H and C=O stretches is consistent with the ring opening of the pyrazolines and enolate form of the amide functionalities in $(H^RL)^{2–}$ (R = H and OMe) and $(^RL–^RL)^{6–}$ (R = H, OMe, and NMe_2). In contrast, complexes **6**–**8** display a medium-intensity band in the range 1647–1650 $cm^{–1}$ due to the presence of the C=O group at the central C atom of the tetradentate ligand $(^RLO)^{2–}$ (Scheme 1). A medium to strong band observed between 1591–1604 $cm^{–1}$ in the spectra of all complexes is most likely due to the conjugated -C=N–N=C- fragment present in all three types of ligands.[4,5,9–11]

Description of the Molecular Structures

The molecular structures of $[Ni(H^RL)]$ [**1** (R = H) and **2** (R = OMe)], $[Ni(^NL–^NL)Ni]$ (**5**, R = NMe_2), and $[Ni(^RLO)]$ [**7** (R = OMe) and **8** (R = NMe_2)] are shown in Figures 1, 2 and 3, respectively. The two halves of the molecule of **1**

are related by a crystallographically imposed twofold axis of symmetry. In each of the remaining structures, a complete molecule of the complex is present in the asymmetric unit. The bond parameters associated with the metal ion in these complex molecules are listed in Tables 1, 2, and 3.

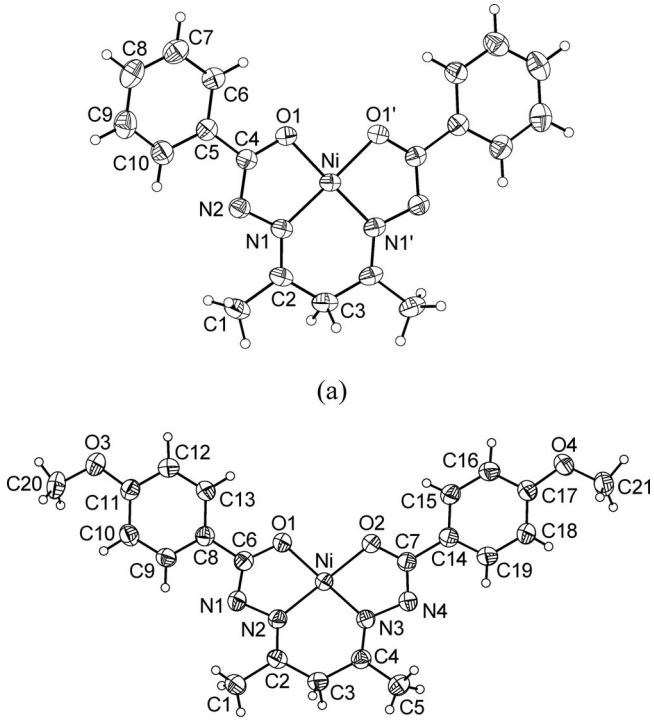

Figure 1. Molecular structures of (a) [Ni(HL)] (**1**, R = H) and (b) [Ni(H^{M}L)] (**2**, R = OMe) with the atom labeling schemes. All non-hydrogen atoms are represented by their 30% and 50% probability thermal ellipsoids for **1** and **2**, respectively.

In **1**, **2**, **7**, and **8**, the C–O and C=N bond lengths in the -(O⁻)C=N- fragments of the ligands are in the ranges 1.288(3)–1.301(2) Å and 1.306(6)–1.331(3) Å, respectively. These bond lengths are consistent with the enolate form of both amide functionalities present in the ligands $[(H^{R}L)^{2-}$ and $(^{R}LO)^{2-}]$.[4,5,9,11] The N=C [1.290(6)–1.304(6) Å] and C–C bond lengths [1.474(6)–1.489(4) Å] in the N=C–C(H_2/O)–C=N fragments of $(H^{R}L)^{2-}$ and $(^{R}LO)^{2-}$ are similar to the corresponding bond lengths reported for analogous tetradentate ligands[5,8,9,11b] and are consistent with the imine and carbon-to-carbon single-bond lengths, respectively. In contrast, the N–C [1.339(3) and 1.352(3) Å] and the C–C [1.394(4) and 1.387(4) Å] bond lengths in the N=C–C(H)=C–N fragment of $(L)^{3-}$ in the previously reported divanadium(IV) complex $[V_2(L)_2(\mu\text{-PhCONNCOPh})]$[9] clearly indicate that the third proton is dissociated here and the resultant additional negative charge is delocalized. The C=O bond lengths in **7** [1.233(5) Å] and **8** [1.225(3) Å] are unexceptional (Figure 3).[5,11b] The Ni–O(amide) [1.8471(18)–1.860(3) Å] and Ni–N(imine) [1.833(4)–1.840(4) Å] bond lengths in these four structures are very similar and comparable with the bond lengths observed in

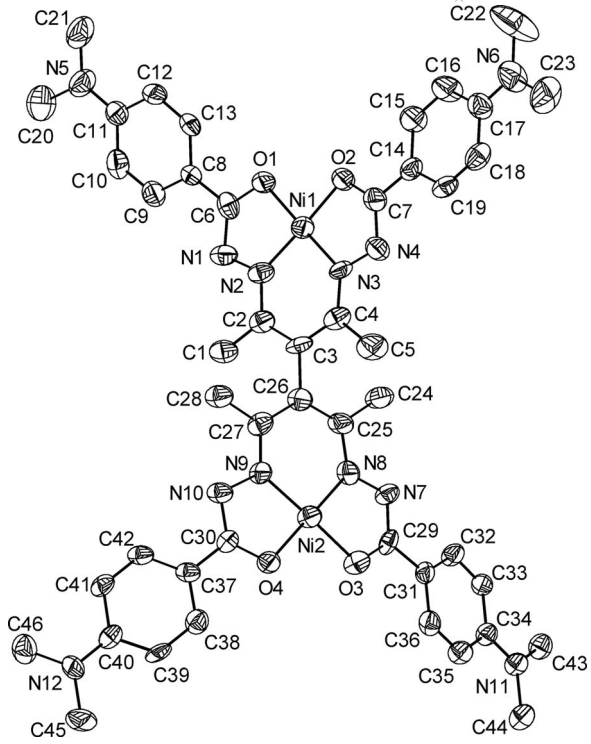

Figure 2. Molecular structure of [Ni(^{N}L–^{N}L)Ni] (**5**, R = NMe_2) with the atom labeling scheme. All atoms are represented by their 30% probability thermal ellipsoids. Hydrogen atoms are omitted for clarity.

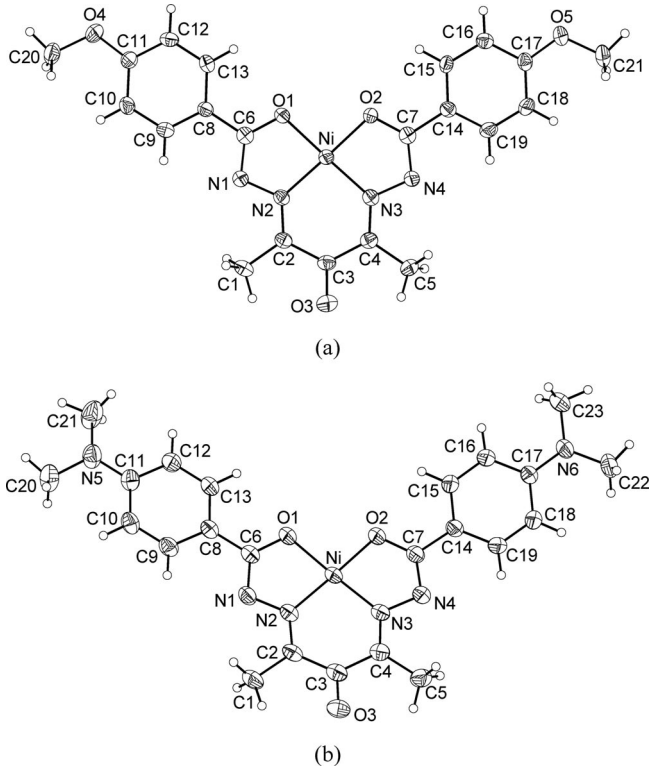

Figure 3. Molecular structures of (a) [Ni(^{M}LO)] (**7**, R = OMe) and (b) [Ni(^{N}LO)] (**8**, R = NMe_2) with the atom labeling schemes. All non-hydrogen atoms are represented by their 30% probability thermal ellipsoids for both structures.

Table 1. Selected bond lengths [Å] and angles [°] for [Ni(HL)]·0.5H_2O (**1**·0.5H_2O) and [Ni(H^ML)] (**2**).

[Ni(HL)]·0.5H_2O (**1**·0.5H_2O)[a]			
Ni–N1	1.833(4)	Ni–N1′	1.833(4)
Ni–O1	1.856(3)	Ni–O1′	1.856(3)
N1′–Ni–N1	96.6(2)	N1–Ni–O1	84.57(16)
N1–Ni–O1′	178.79(16)	N1′–Ni–O1	178.79(16)
N1′–Ni–O1′	84.57(16)	O1–Ni–O1′	94.22(19)
[Ni(H^ML)] (**2**)			
Ni–N2	1.8344(15)	Ni–N3	1.8366(15)
Ni–O1	1.8586(13)	Ni–O2	1.8600(13)
N2–Ni–N3	96.18(7)	N2–Ni–O1	84.43(6)
N2–Ni–O2	179.59(6)	N3–Ni–O1	177.73(6)
N3–Ni–O2	84.16(6)	O1–Ni–O2	95.23(5)

[a] Symmetry operation used to generate equivalent atoms: x, y + 1/2, $-z$ + 1/2.

Table 2. Selected bond parameters for [Ni(^NL–^NL)Ni]·$(CH_3)_2CO$ {**5**·$(CH_3)_2CO$}.

Bond lengths [Å]			
Ni1–N2	1.803(9)	Ni2–N8	1.821(8)
Ni1–N3	1.806(8)	Ni2–N9	1.821(8)
Ni1–O1	1.845(6)	Ni2–O3	1.846(6)
Ni1–O2	1.843(7)	Ni2–O4	1.856(6)
Bond angles [°]			
N2–Ni1–N3	97.3(5)	N8–Ni2–N9	95.6(4)
N2–Ni1–O1	84.4(4)	N8–Ni2–O3	84.7(4)
N2–Ni1–O2	177.9(4)	N8–Ni2–O4	177.2(3)
N3–Ni1–O1	177.7(4)	N9–Ni2–O3	175.9(3)
N3–Ni1–O2	84.7(4)	N9–Ni2–O4	84.2(4)
O1–Ni1–O2	93.5(3)	O3–Ni2–O4	95.2(3)

Table 3. Selected bond lengths [Å] and angles [°] for [Ni(^MLO)] (**7**) and [Ni(^NLO)]·$CHCl_3$ (**8**·$CHCl_3$).

Complex	**7**	**8**·$CHCl_3$
Ni–N2	1.840(4)	1.837(2)
Ni–N3	1.833(4)	1.838(2)
Ni–O1	1.856(3)	1.8551(19)
Ni–O2	1.860(3)	1.8471(18)
N2–Ni–N3	96.52(17)	97.47(9)
N2–Ni–O1	84.52(15)	84.37(9)
N2–Ni–O2	178.67(16)	178.07(9)
N3–Ni–O1	177.88(15)	178.08(8)
N3–Ni–O2	84.58(15)	84.35(8)
O1–Ni–O2	94.40(13)	93.82(8)

nickel(II) complexes having the same coordinating atoms.[4c,5,8,11] In all four structures, there is no displacement of the metal center from the N_2O_2 square plane around it. The mean deviations from the plane constituted by the nickel, two imine N, and two amide O atoms are within 0.002–0.019 Å. In fact, all the atoms that constitute the three chelate rings including the two methyl C atoms attached to the imine groups are satisfactorily planar (mean deviations 0.028–0.037 Å). However, none of the four molecules is perfectly planar, because of the rotation of the aromatic ring planes around the C–C bonds that connect them to the amide C atoms in the aroyl fragments of the tetradentate ligand. As the two halves of the molecule of **1** are related by a twofold axis of symmetry (Figure 1), the dihedral angles between the aromatic ring planes and the plane containing the three chelate rings have the same value of 4.6(2)°, while the corresponding dihedral angles in **2** are 17.96(5)° and 2.41(8)°. On the other hand, these dihedral angles are 2.9(2)° and 8.8(2)° in **7**, and 3.4(1)° and 7.7(1)° in **8**.

The C–O [1.290(12)–1.314(11) Å] and C=N bond lengths [1.317(12)–1.343(13) Å] in the -(O^-)C=N- fragments of the ligand in [Ni(^NL–^NL)Ni] (**5**) (Figure 2) are slightly longer than the corresponding bond lengths observed in **1**, **2**, **7**, and **8**. However, they are within the range reported for the enolate form of the O-coordinating amide functionalities.[4,5,9,11] The Ni–O(amide) bond lengths [1.843(7)–1.856(6) Å] in **5** are marginally shorter than those in **1**, **2**, **7**, and **8**. The N–C and the C–C bond lengths in the N=C–C=C=N fragments of (^NL–^NL)$^{6-}$ are in the ranges 1.311(12)–1.353(11) Å and 1.400(13)–1.445(14) Å, respectively. Thus the N–C bonds are longer and the C–C bonds are shorter in **5** than the corresponding bonds in **1**, **2**, **7**, and **8**, and they are comparable with the corresponding bonds reported for [V_2(L)$_2$(μ-PhCONNCOPh)].[9] Therefore, the third negative charge in each half of (^NL–^NL)$^{6-}$ is delocalized over the N=C=C=C=N fragment. The corresponding significantly shorter N=C [1.285(4) and 1.290(4) Å] and longer C–C [1.518(5)(4) and 1.507(5) Å] bonds in the centrosymmetric [OV^{IV}(HL–LH)$V^{IV}O$][9] (Scheme 1) further corroborate the presence and delocalization of the additional charges in the central part of (^NL–^NL)$^{6-}$ in **5**. Thus, both metal ions are in the +3 formal oxidation state in **5**. This is also reflected in the significantly shorter Ni–N bond lengths [1.803(9)–1.821(8) Å] in **5** relative to the Ni–N(imine) bond lengths observed in **1**, **2**, **7**, and **8**. As observed in the other structures, there is no displacement of the metal centers from the N_2O_2 square planes. The mean deviations from the planes constituted by NiN_2O_2 are 0.01 and 0.02 Å. In each of the two halves of the dinuclear molecule, the three chelate rings including the two methyl C atoms of the imine groups are satisfactorily planar (mean deviations 0.03 and 0.08 Å). The dihedral angle between these two planes is 67.4(1)°. Thus the molecule is twisted along the C3–C26 single bond [1.486(13) Å] that acts as the bridge between its two halves (Figure 2). The aromatic ring planes of the aroyl fragments are also twisted along the (ring)C–C(amide) bonds. In the first half of the molecule, the dihedral angles between these ring planes and the plane containing the three chelate rings are 6.8(6)° and 13.3(5)°, while in the second half of the molecule these dihedral angles are 21.0(4)° and 18.2(3)°.

In the solid state, square-planar complexes of bivalent nickel and copper often exist as dimeric units or polymeric chains due to coordination of a metal-coordinated atom of an adjacent molecule at the apical site.[12] Scrutiny of the crystal packing reveals that none of complexes **1**, **2**, **7**, and **8** forms a dimer or a polymer due to such equatorial–apical bridging. However, the dinuclear molecules of **5** exist as dis-

crete centrosymmetric dimeric units (Figure 4) in the crystal lattice due to formation of two reciprocal equatorial–apical bridges between the two halves of the two dinuclear molecules involving one of the two metal-coordinated amide O atoms [O3] of each half. The Ni2···O3′ distance is 3.300(7) Å, and the four angles formed by O3′ with the four atoms of the N_2O_2 square plane at Ni2 are in the range 85.3(3)°–97.5(2)°. These parameters indicate a weak coordination of the amide O atom at the apical site of the metal center. The Ni2···Ni2′ distance and the Ni2···O3′···Ni2′ bridging angle are 3.631(3) Å and 84.8(2)°, respectively. The asymmetric unit of the previously reported analogous dinuclear complex [Ni(L^2–L^2)Ni] (Scheme 1) contains two molecules.[8] It may be noted that one of them also forms discrete dimers as observed for **5**, and the other one forms infinite chains due to the uneven stacking of the two halves of each dinuclear molecule with the two halves of the two adjacent dinuclear molecules.[8] Here the intermolecular Ni···Ni distances are shorter than that in **5**. The Ni···Ni distances are 3.202 and 3.617 Å in the infinite chain, while the corresponding value is 3.402 Å in the dimer. The metal centers in [Ni(L^2–L^2)Ni] are in the N_4 square plane, and the stacking of the molecules is believed to be due to both metal–metal bonding and π–π interaction between the ligands.

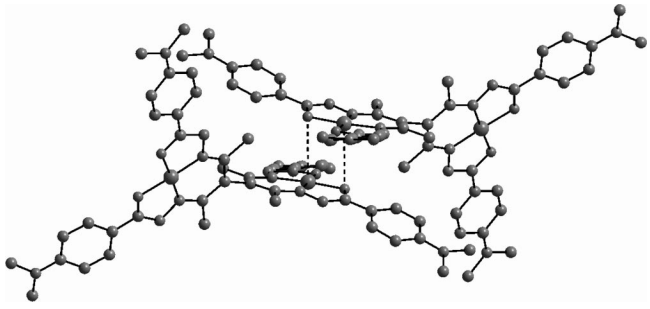

Figure 4. Dimer of [Ni(^{N}L–^{N}L)Ni] (**5**, R = NMe_2) formed by means of equatorial–apical bridging.

Magnetic Susceptibilities

The diamagnetic character of **1**, **2**, and **6**–**8** is consistent with the square-planar coordination geometry and the +2 oxidation state of the nickel in each of these complexes. In contrast, complexes **3**–**5** are paramagnetic. The magnetic moments of these species at 300 K are in the range 2.47–2.55 μ_B. These values are essentially the spin-only values expected for dinuclear nickel(III) species. To examine whether there is any spin coupling, we have measured the magnetic susceptibilities of **3** in the temperature range 2–300 K at a constant magnetic field of 5 kG. The curves obtained by plotting the effective magnetic moment (μ_{eff}) and inverse molar magnetic susceptibility values against temperature are shown in Figure 5. The μ_{eff} at 300 K is 2.55 μ_B. On cooling, the moment gradually decreases, and the μ_{eff} at 2 K is 1.94 μ_B. The nature of the curve clearly indicates a small but definite antiferromagnetic interaction in **3**. The data were fitted by using the expression for χ_M vs. T derived from the isotropic spin-exchange Hamiltonian $H = -2JS_1 \cdot S_2$, where $S_1 = S_2 = 1/2$.[13] The best least-squares fit[14] (Figure 5) was obtained with $J = -1.4(1)$ cm^{-1} and $g = 2.079(1)$. Perhaps this weak antiferromagnetic spin coupling in **3** is mainly through the equatorial–apical bridges as observed in the crystal structure of **5**, or, in other words, due to intermolecular interactions. Such weak spin coupling is very common in species containing equatorial–apical bridges.[12] In contrast, the cryomagnetic studies showed that the antiferromagnetic coupling is much stronger in the analogous species [Ni(L^2–L^2)Ni][8] than that in **3**. Here the inter- as well as intramolecular interactions are considered as the primary reasons for the strong spin coupling.

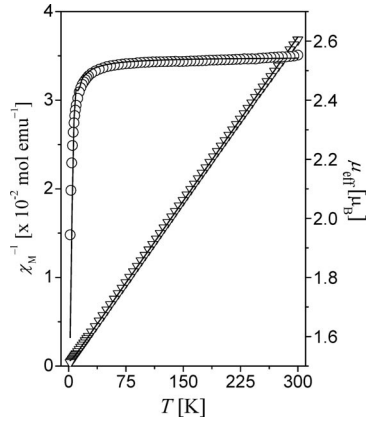

Figure 5. Temperature dependence of inverse molar magnetic susceptibilities (▽) and effective magnetic moments (O) of [Ni(L–L)Ni] (**3**, R = H). The solid lines were generated from the best least-squares fit parameters given in the text.

EPR Spectra

Tetradentate Schiff base ligands similar to the ligands in **3**–**5** derived from acetylacetone are known to behave as noninnocent ligands.[8,15] As reported in our earlier paper,[5] we have collected the EPR spectra of **4** and **5** and compared them with the spectra of **3** to understand whether these complexes are authentic nickel(III) species or nickel(II)-stabilized ligand radical systems. At 300 K, all the complexes in the powder phase display an isotropic signal at $g \approx 2.0$ with a peak-to-peak separation around 70–80 G. These peak-to-peak separation values are significantly larger than the values expected for ligand radical systems.[16] However, dichloromethane solutions of the complexes at room temperature display isotropic signals at $g \approx 2.1$ but with much smaller peak-to-peak separations (17–25 G) relative to that observed in the room-temperature powder spectra. In contrast, the spectra of all three complexes at 115 K in the powder phase as well as in frozen dichloromethane are rhombic in character (Table 4).[5] The low-temperature powder spectra of **4** and **5** are shown in Figure 6. The resolution of g_1 for **5** and that of both g_1 and g_3 for **4** are not as good as

that observed for **3**.[5] In frozen (115 K) dichloromethane solution, g_1 and g_3 are marginally better resolved for **4** than that observed in its powder spectrum. On the other hand, the highest field signal is significantly broadened for each of **3**[5] and **5**. The g_{av} values (2.00–2.01) calculated from all the rhombic spectra of **3**–**5** are very similar to the values reported for nickel(II)-stabilized ligand radical systems.[16] It may be noted that none of the fluid or frozen solution spectra display nitrogen hyperfine structure. Thus, except for the g values, the other EPR spectral features do not conclusively indicate that complexes **3**–**5** are nickel(II)-stabilized ligand radical systems. On the other hand, a rhombic EPR spectrum is not unusual for square-planar nickel(III) species due to distortion or weak apical coordination.[3a,16e] Perhaps a borderline situation between the authentic nickel(III) and the nickel(II)-stabilized ligand radical system is the best description for complexes **3**–**5**.

Table 4. EPR spectroscopic data at 115 K.

Complex	Phase	g values
[Ni(L–L)Ni] (**3**)	powder	2.02, 2.01, 1.98
	dichloromethane	2.02, 2.01, 1.98
[Ni(^{M}L–^{M}L)Ni] (**4**)	powder	2.02, 2.01, 1.98
	dichloromethane	2.02, 2.00, 1.98
[Ni(^{N}L–^{N}L)Ni] (**5**)	powder	2.01, 2.00, 1.98
	dichloromethane	2.02, 2.01, 1.99

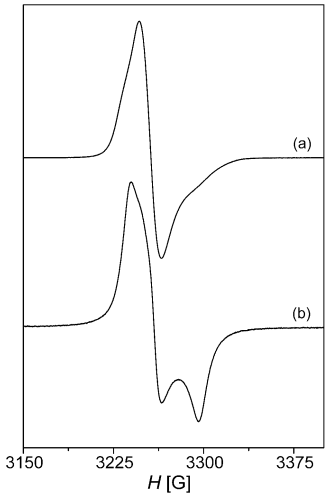

Figure 6. EPR spectra of (a) [Ni(^{M}L–^{M}L)Ni] (**4**, R = OMe) and (b) [Ni(^{N}L–^{N}L)Ni] (**5**, R = NMe_2) in the powder phase at 115 K.

Conclusions

We have described three different types of nickel complexes with the tetradentate Schiff base system acetylacetone bis(4-R-benzoylhydrazone) ($H_3{}^{R}$L, where the 3 H atoms represent the dissociable protons of the two amide functionalities and the active methylene group) expected to be formed by the reaction of acetylacetone with 4-R-benzoylhydrazine in a 1:2 mol ratio. Two of them are mononuclear square-planar nickel(II) complexes, [Ni(H^{R}L)] and its oxidized product [Ni(^{R}LO)], and the third type is a formally dinickel(III) species, [Ni(^{R}L–^{R}L)Ni]. The sequence of conversion from one type to the other is [Ni(H^{R}L)] → [Ni(^{R}L–^{R}L)Ni] → [Ni(^{R}LO)]. Earlier reports[6d,7,8] on nickel complexes with similar ligands describe complexes analogous to [Ni(H^{R}L)] and their conversion to either [Ni(^{R}LO)] or [Ni(^{R}L–^{R}L)Ni] types of species. In this work, we have been able to establish the links between these three types of complexes. The nickel(II) complex, [Ni(H^{R}L)], that formed first undergoes a $4e^-$ and $2H^+$ oxidation in the presence of oxy-

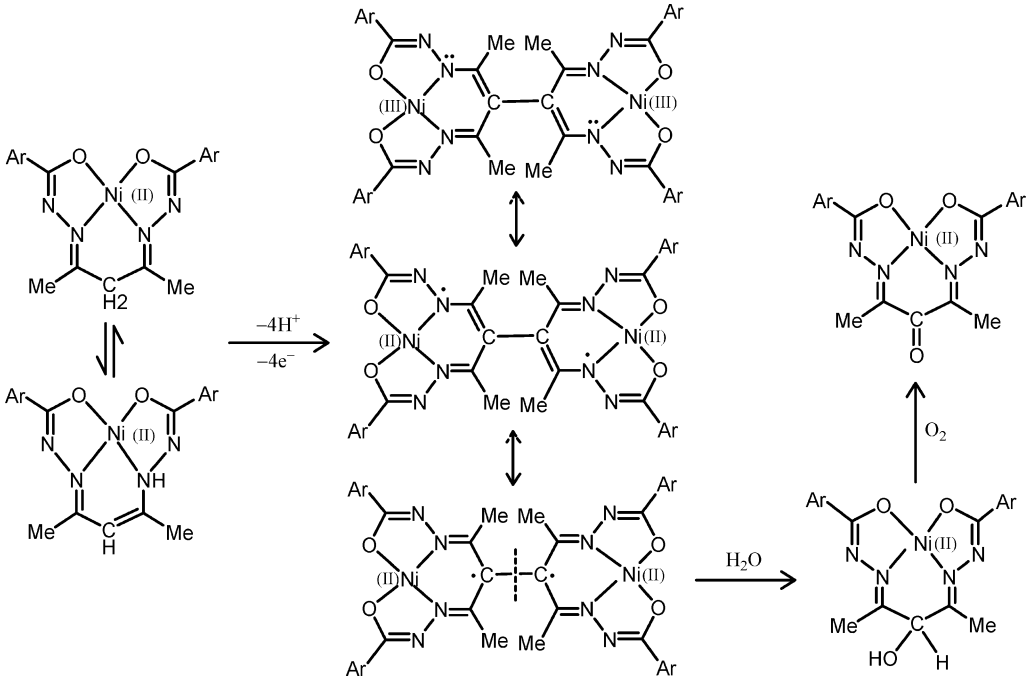

Scheme 2. A plausible mechanism for the [Ni(H^{R}L)] → [Ni(^{R}L–^{R}L)Ni] → [Ni(^{R}LO)] process.

gen to provide the paramagnetic dinuclear complex [Ni(^{R}L–^{R}L)Ni], which is transformed to a new nickel(II) complex, [Ni(^{R}LO)], in the presence of both water and oxygen (Scheme 2). Considering the mechanisms suggested[17] for the metal-assisted conversion of a methine group to a keto group and the borderline nature of [Ni(^{R}L–^{R}L)Ni], a speculative mechanism for the formation of [Ni(^{R}LO)] from it is as follows: localization of two unpaired electrons on the bridging C–C atoms, homolytic cleavage of the C–C bond, addition of water to form -CH(OH)-, and finally 2e and $2H^+$ oxidation by oxygen to the keto group (Scheme 2).

Experimental Section

Materials: All the chemicals and solvents used in this work were of analytical grade, they were available commercially and were used without further purification.

Physical Measurements: Elemental analysis data were obtained with a Thermo Finnigan Flash EA1112 series elemental analyzer. Solution electrical conductivities were measured with a Digisun DI-909 conductivity meter. A Jasco-5300 FTIR spectrophotometer was used to record the infrared spectra of the complexes in KBr disks. A Jeol JES-FA200 spectrometer was used for EPR experiments. Room-temperature (300 K) magnetic susceptibility data were collected with the help of a Sherwood Scientific balance. A SQUID magnetometer was used for the variable-temperature (2–300 K) magnetic susceptibility measurements. Diamagnetic corrections calculated from Pascal's constants[18] were used to obtain the molar paramagnetic susceptibilities.

Synthesis of the Complexes

[Ni(HL)]·0.5H$_2$O (1·0.5H$_2$O): To a methanol solution (20 mL) of bzpyzn (572 mg, 1.7 mmol) was added dropwise a methanol solution (20 mL) of Ni(O$_2$CCH$_3$)$_2$·4H$_2$O (425 mg, 1.7 mmol) over a period of 5 min with stirring. The mixture was heated to reflux for 1 h. The brown crystalline complex that separated on cooling to room temperature was collected by filtration, washed with methanol, and dried in vacuo over anhydrous CaCl$_2$. Yield: 470 mg (69%). $C_{19}H_{19}N_4O_{2.5}Ni$ (402.09): calcd. C 56.76, H 4.76, N 13.93; found C 56.45, H 4.58, N 13.71.

[Ni(H^{M}L)] (2): Acetylacetone (170 mg, 1.7 mmol) was added to a methanol solution (20 mL) of 4-methoxybenzoylhydrazine (565 mg, 3.4 mmol), and the mixture was heated to reflux for 1 h. A methanol solution (20 mL) of Ni(O$_2$CCH$_3$)$_2$·4H$_2$O (425 mg, 1.7 mmol) was added dropwise over a period of 5 min to the above mixture followed by heating to reflux for 1 h. On cooling to room temperature, the complex was separated as a brown crystalline material. It was collected by filtration, washed with methanol, and dried in vacuo over anhydrous CaCl$_2$. Yield: 500 mg (65%). $C_{21}H_{22}N_4O_4Ni$ (453.14): calcd. C 55.67, H 4.89, N 12.36; found C 55.52, H 4.73, N 12.24.

[Ni(L–L)Ni] (3): This complex[5] was prepared in 75% yield by using the same reagents, same solvent, and a very similar procedure as that described for **1**. The only difference in this preparation was that the reaction mixture was stirred in air at room temperature for 5 h instead of heating to reflux for 1 h. $C_{38}H_{32}N_8O_4Ni_2$ (782.10): calcd. C 58.36, H 4.12, N 14.33; found C 57.85, H 4.25, N 14.07.[5]

[Ni(^{M}L–^{M}L)Ni] (4): This complex was prepared in 72% yield by using the same reagents, same solvent, and a very similar procedure as that described for **2**. However, in this case, after addition of Ni(O$_2$CCH$_3$)$_2$·4H$_2$O the reaction mixture was stirred in air at room temperature for 5 h instead of heating to reflux for 1 h. $C_{42}H_{40}N_8O_8Ni_2$ (902.21): calcd. C 55.91, H 4.47, N 12.42; found C 55.68, H 4.31, N 12.29.

[Ni(^{N}L–^{N}L)Ni] (5): This complex was prepared in 80% yield by using 4-*N*,*N*-dimethylbenzoylhydrazine and the same procedure as that described for **4**. $C_{46}H_{52}N_{12}O_4Ni_2$ (954.37): calcd. C 57.89, H 5.49, N 17.61; found C 57.62, H 5.35, N 17.44.

[Ni(LO)] (6), [Ni(^{M}LO)] (7) and [Ni(^{N}LO)] (8): Complex **6** was prepared from **3** as reported before.[5] Complexes **7** and **8** were prepared in approximately 20% yields from **4** and **5**, respectively. The procedures were very similar to that used for **6**. $C_{21}H_{20}N_4O_5Ni$ {[Ni(^{M}LO)] (**7**)} (467.10): calcd. C 54.00, H 4.32, N 11.99; found C 53.78, H 4.26, N 11.87. $C_{23}H_{26}N_6O_3Ni$ {[Ni(^{N}LO)] (**8**)} (493.10): calcd. C 56.01, H 5.31, N 17.04; found C 55.84, H 5.10, N 16.78.

X-ray Crystallography: Single crystals of **1**·0.5H$_2$O, **2**, and **7** were collected directly from the materials obtained during their syntheses. Single crystals of **5** were obtained as **5**·(CH$_3$)$_2$CO by slow evaporation of an acetone solution. Complex **8** crystallizes from chloroform solution as **8**·CHCl$_3$. For all the crystals, the unit cell param-

Table 5. Crystallographic data for **1**·0.5H$_2$O, **2**, **5**·(CH$_3$)$_2$CO, **7**, and **8**·CHCl$_3$.

Complex	**1**·0.5H$_2$O	**2**	**5**·(CH$_3$)$_2$CO	**7**	**8**·CHCl$_3$
Chemical formula	$C_{19}H_{19}N_4O_{2.5}Ni$	$C_{21}H_{22}N_4O_4Ni$	$C_{49}H_{58}N_{12}O_5Ni_2$	$C_{21}H_{20}N_4O_5Ni$	$C_{24}H_{27}N_6O_3Cl_3Ni$
Formula weight [g mol^{-1}]	402.09	453.14	1012.49	467.12	612.57
Crystal system	orthorhombic	monoclinic	monoclinic	monoclinic	monoclinic
Space group	*Ccca*	$P2_1/c$	$P2_1/c$	$P2_1/n$	$P2_1/n$
a [Å]	20.719(2)	7.7101(7)	15.084(3)	7.9947(15)	17.2579(12)
b [Å]	23.480(2)	11.9373(10)	24.334(5)	16.915(3)	7.8024(5)
c [Å]	7.5740(7)	21.2125(18)	14.952(3)	14.735(3)	21.1395(14)
β [°]	–	93.052(1)	118.669(3)	93.714(4)	102.176(1)
V [Å^3]	3684.6(6)	1949.6(3)	4815.4(16)	1988.4(6)	2782.5(3)
Z	8	4	4	4	4
μ [mm^{-1}]	1.077	1.033	0.842	1.019	1.022
Measured reflections	9543	19748	36566	18891	27836
Unique reflections	1814	3827	6299	3511	5457
Reflections $I \geq 2\sigma_I$	1378	3382	2419	2290	4395
Parameters	123	281	627	284	340
GOF on F^2	1.103	1.061	0.957	1.054	1.036
$R1$, $wR2$ ($I \geq 2\sigma_I$)	0.0706, 0.1608	0.0310, 0.0782	0.0796, 0.1371	0.0651, 0.1140	0.0475, 0.1273
$\Delta\rho_{max}$, $\Delta\rho_{min}$ [e Å^{-3}]	1.040, –0.529	0.246, –0.367	0.289, –0.350	0.467, –0.264	0.471, –0.431

eters and the intensity data were obtained with a Bruker-Nonius SMART APEX CCD single-crystal X-ray diffractometer, equipped with a graphite monochromator and a Mo-K_α fine-focus sealed tube (λ = 0.71073 Å), operated at 2.0 kW. The detector was placed at a distance of 6.0 cm from the crystal. Data were collected at 298 K with a scan width of 0.3° in ω and an exposure time of 10 s/frame. The SMART software was used for data acquisition and the SAINT-Plus software was used for data reduction.[19] The SADABS program[20] was used for the absorption correction. In each case, the structure was solved by direct methods and refined on F^2 by full-matrix least-squares procedures. All non-hydrogen atoms were refined anisotropically. In the case of **1**·0.5H_2O, the asymmetric unit contains half of the complex molecule and one quarter of a water molecule. The hydrogen atom of the disordered water molecule was located in a difference map and included in the structure factor calculation with geometric restraints. The remaining hydrogen atoms in **1**·0.5H_2O and all hydrogen atoms in **2**, **5**·$(CH_3)_2CO$, **7**, and **8**·$CHCl_3$ were added at idealized positions by using a riding model. The SHELX-97 programs[21] of the WinGX package[22] were used for structure solution and refinement. The ORTEX6a[23] and Platon[24] packages were used for the molecular graphics. Selected crystallographic data for all the structures are listed in Table 5. CCDC-729266 (for **1**·0.5H_2O), -729267 (for **2**), -729268 {for **5**·$(CH_3)_2CO$}, -729269 (for **7**), -729270 {for **8**·$CHCl_3$} contain the supplementary crystallographic data for this paper. These data can be obtained free of charge from The Cambridge Crystallographic Data Centre via www.ccdc.cam.ac.uk/data_request/cif.

Acknowledgments

Financial assistance received from the Department of Science and Technology (DST), New Delhi (Grant No. SR/S1/IC-10/2007) is gratefully acknowledged. A. Mukhopadhyay thanks the Council of Scientific and Industrial Research, New Delhi, for a research fellowship. Our sincere thanks are due to Prof. Wataru Fujita for providing the cryomagnetic data. X-ray structures were determined at the National Single Crystal Diffractometer Facility, School of Chemistry, University of Hyderabad (established by the DST). We thank the University Grants Commission, New Delhi, for the facilities provided under the UPE and CAS programs.

[1] a) H. Yoon, T. R. Wagler, K. J. O'Connor, C. J. Burrows, *J. Am. Chem. Soc.* **1990**, *112*, 4568; b) L. P. Tikhonova, S. V. Rosokha, E. A. Bakay, *React. Kinet. Catal. Lett.* **1998**, *63*, 129; c) J. M. Grill, J. W. Ogle, S. A. Miller, *J. Org. Chem.* **2006**, *71*, 9291; d) R. Cammack, *Adv. Inorg. Chem.* **1988**, *32*, 297; e) D. P. Mack, P. B. Dervan, *J. Am. Chem. Soc.* **1990**, *112*, 4604; f) *The Bioinorganic Chemistry of Nickel* (Ed.: J. R. Lancaster), VCH, New York, **1988**; g) A. E. Przybyla, J. Robbins, N. Menon, H. D. Peck Jr, *FEMS Microbiol. Lett.* **1992**, *88*, 109; h) E. Bouwman, J. Reedijk, *Coord. Chem. Rev.* **2005**, *249*, 1555.

[2] a) K. Nag, A. Chakravorty, *Coord. Chem. Rev.* **1980**, *33*, 87; b) S. Bhattacharya, R. Mukherjee, A. Chakravorty, *Inorg. Chem.* **1986**, *25*, 3448; c) D. Ray, A. Chakravorty, *Inorg. Chem.* **1988**, *27*, 3292; d) A. G. Lappin, A. McAuley, *Adv. Inorg. Chem.* **1988**, *32*, 241; e) S. Bhattacharya, B. Saha, A. Dutta, P. Banerjee, *Coord. Chem. Rev.* **1998**, *170*, 47.

[3] a) T. J. Collins, T. R. Nichols, E. S. Uffelman, *J. Am. Chem. Soc.* **1991**, *113*, 4708; b) D. W. Margerum, *Pure Appl. Chem.* **1983**, *32*, 297.

[4] a) R. Raveendran, S. Pal, *Eur. J. Inorg. Chem.* **2008**, 5540; b) R. Raveendran, S. Pal, *Inorg. Chim. Acta* **2007**, *692*, 824; c) A. Mukhopadhyay, S. Pal, *Eur. J. Inorg. Chem.* **2006**, 4879; d) S. Das, S. Pal, *J. Mol. Struct.* **2005**, *741*, 183; e) S. Das, S. Pal, *J. Organomet. Chem.* **2004**, *689*, 352; f) S. N. Pal, S. Pal, *Eur. J. Inorg. Chem.* **2003**, 4244; g) S. N. Pal, S. Pal, *J. Chem. Soc., Dalton Trans.* **2002**, 2102; h) S. Pal, *Proc. Indian Acad. Sci. (Chem. Sci.)* **2002**, *114*, 417; i) S. N. Pal, K. R. Radhika, S. Pal, *Z. Anorg. Allg. Chem.* **2001**, *627*, 1631; j) N. R. Sangeetha, S. Pal, *Bull. Chem. Soc. Jpn.* **2000**, *73*, 357; k) N. R. Sangeetha, C. K. Pal, P. Ghosh, S. Pal, *J. Chem. Soc., Dalton Trans.* **1996**, 3293.

[5] A. Mukhopadhyay, S. Pal, *Polyhedron* **2004**, *23*, 1997.

[6] a) H. Buttkus, R. J. Bose, *J. Org. Chem.* **1971**, *36*, 3895; b) D. H. Hunter, C. McRoberts, J. J. Vittal, *Can. J. Chem.* **1998**, *76*, 522; c) E. C. Constable, M. J. Doyle, S. M. Elder, P. R. Raithby, *J. Chem. Soc., Chem. Commun.* **1989**, 1376; d) S. C. Davies, M. C. Durrant, D. L. Hughes, A. Pezeshk, R. L. Richards, *J. Chem. Res. (S)* **2001**, 100.

[7] V. B. Arion, N. V. Gerbeleu, K. M. Indrichan, *Russ. J. Inorg. Chem.* **1985**, *30*, 70.

[8] V. Arion, K. Wieghardt, T. Weyhermueller, E. Bill, V. Leovac, A. Rufinska, *Inorg. Chem.* **1997**, *36*, 661.

[9] K. Kopka, R. Mattes, *Z. Naturforsch. Teil B* **1995**, *50*, 1281.

[10] S. G. Sreerama, S. Pal, *Inorg. Chem.* **2005**, *44*, 6299.

[11] a) K. C. Joshi, R. Bohra, B. S. Joshi, *Inorg. Chem.* **1992**, *31*, 598; b) H. Yin, S.-X. Liu, *Chin. J. Inorg. Chem.* **2002**, *18*, 269; c) A. Mukhopadhyay, G. Padmaja, S. N. Pal, S. Pal, *Inorg. Chem. Commun.* **2003**, *6*, 381.

[12] a) F. A. Cotton, G. Wilkinson, *Advanced Inorganic Chemistry*, Wiley, New York, **1980**, p. 793; b) N. R. Sangeetha, S. Pal, *Polyhedron* **2000**, *19*, 1593.

[13] C. J. O'Connor, *Prog. Inorg. Chem.* **1982**, *29*, 203.

[14] G. V. R. Chandramouli, C. Balagopalakrishna, M. V. Rajasekharan, P. T. Manoharan, *Comput. Chem.* **1996**, *20*, 353.

[15] U. Knof, T. Weyhermüller, T. Wolter, K. Wieghardt, E. Bill, C. Butzlaff, A. X. Trautwein, *Angew. Chem. Int. Ed. Engl.* **1993**, *32*, 1635.

[16] a) J. A. McCleverty, *Prog. Inorg. Chem.* **1968**, *10*, 49; b) R. S. Drago, I. Baucom, *Inorg. Chem.* **1972**, *11*, 2064; c) R. R. Gagne, D. M. Ingle, *Inorg. Chem.* **1981**, *20*, 420; d) K. Weighardt, W. Walz, B. Nuber, J. Weiss, A. Ozarowski, H. Stratemeier, D. Reinen, *Inorg. Chem.* **1986**, *25*, 1650; e) Y. Shimazaki, F. Tani, K. Fukui, Y. Naruta, O. Yamauchi, *J. Am. Chem. Soc.* **2003**, *125*, 10512.

[17] a) K. C. Cariepy, M. A. Curtin, M. J. Clarke, *J. Am. Chem. Soc.* **1989**, *111*, 4947; b) S. Choi, S. Delaney, L. Orbai, E. J. Padgett, A. S. Hakemian, *Inorg. Chem.* **2001**, *40*, 5481.

[18] W. E. Hatfield, *Theory and Applications of Molecular Paramagnetism* (Eds.: E. A. Boudreaux, L. N. Mulay), Wiley, New York, **1976**, p. 491.

[19] *SMART 5.630 and SAINT-plus 6.45*, Bruker-Nonius Analytical X-ray Systems Inc., Madison, WI, USA, **2003**.

[20] G. M. Sheldrick, *SADABS Program for Area Detector Absorption Correction*, University of Göttingen, Göttingen, Germany, **1997**.

[21] G. M. Sheldrick, *SHELX-97 Programs for Crystal Structure Analysis*, University of Göttingen, Göttingen, Germany, **1997**.

[22] L. J. Farrugia, *J. Appl. Crystallogr.* **1999**, *32*, 837.

[23] P. McArdle, *J. Appl. Crystallogr.* **1995**, *28*, 65.

[24] A. L. Spek, *PLATON A Multipurpose Crystallographic Tool*, Utrecht University, Utrecht, The Netherlands, **2002**.

Received: May 23, 2009
Published Online: August 12, 2009

